

# A series of pyrazolone lanthanide (III) complexes: Synthesis, crystal structures and fluorescence

Jun Li, Li Zhang, Lang Liu, Guangfei Liu, Dianzeng Jia \*, Guancheng Xu

*Institute of Applied Chemistry, Xinjiang University, No. 14 Shengli Road, Urumqi, Xinjiang Province 830046, China*

Received 14 July 2006; received in revised form 18 October 2006; accepted 19 October 2006

Available online 25 October 2006

## Abstract

A series of pyrazolone lanthanide complexes:  $\text{Ln}(\text{PMPP})_3 \cdot 2\text{H}_2\text{O} \cdot \text{C}_2\text{H}_5\text{OH}$  ( $\text{Ln} = \text{Nd}$  (1),  $\text{Sm}$  (2),  $\text{Gd}$  (3),  $\text{Dy}$  (4);  $\text{PMPP} = 1$ -phenyl-3-methyl-4-propionyl-5-pyrazolone) have been synthesized by the hydrothermal method with the starting ligand  $\text{PMPP-SAH}$  (1-phenyl-3-methyl-4-(salicylidene hydrazone)-propionyl-5-pyrazolone) changed into  $\text{PMPP}$  during the formation process of complexes. All the complexes were structurally characterized by X-ray crystallography. The fluorescence of these four complexes 1–4 in solid state and DMF solution was investigated via F-4500 spectrophotometer and all of them indicate a fluorescent behavior at room temperature.

© 2006 Elsevier B.V. All rights reserved.

**Keywords:** Lanthanide; Derivatives of pyrazolone; Crystal structures; Fluorescence

## 1. Introduction

Investigation on molecular coordination compounds of lanthanide ions has been attracted significant attention, owing to their fluorescent broad applications in biochemistry, material chemistry, medicine and so forth [1–4]. Among them, rare earth  $\beta$ -diketonate complexes are a kind of high functional compounds with outstanding optical properties which can be used as fluorescence probes [5–7]. Since,  $\beta$ -diketonate coordination with lanthanide (III) ions has undergone a great proliferation in recent years.

Meanwhile, 4-acyl-pyrazolone derivatives are widely used in many fields in the society, especially clinical and analytical applications [8–10], because pyrazolone, especially 4-acyl-pyrazolone, displays several different coordination modes, with respect to classical  $\beta$ -diketonate [11–13]. In our previous work, we have investigated the synthesis and crystal structure of several derivatives of pyrazolone transition metal complexes [14–16].

To amplify the scope of derivatives of pyrazolone coordinated with rare earth, our group focuses much effort on synthesizing new derivatives of pyrazolone lanthanide complexes, studying on their crystal structures and fluorescent properties. We choose the derivatives of pyrazolone  $\text{PMPP-SAH}$  (1-phenyl-3-methyl-4-(salicylidene hydrazone)-propionyl-5-pyrazolone) coordinated with lanthanide ions, while, what amazed us is that the starting ligand  $\text{PMPP-SAH}$  had been changed into  $\text{PMPP}$  during the formation process of  $\text{Ln}(\text{PMPP})_3 \cdot 2\text{H}_2\text{O} \cdot \text{C}_2\text{H}_5\text{OH}$  ( $\text{Ln} = \text{Nd}$  (1),  $\text{Sm}$  (2),  $\text{Gd}$  (3),  $\text{Dy}$  (4);  $\text{PMPP} = 1$ -phenyl-3-methyl-4-propionyl-5-pyrazolone) and found that these complexes showed interesting structures and fluorescence (see Chart 1).

## 2. Experimental

### 2.1. Syntheses

$\text{Nd}(\text{NO}_3)_3 \cdot 5\text{H}_2\text{O}$ ,  $\text{Sm}(\text{NO}_3)_3 \cdot 6\text{H}_2\text{O}$ ,  $\text{Gd}(\text{NO}_3)_3 \cdot 6\text{H}_2\text{O}$ ,  $\text{Dy}(\text{NO}_3)_3 \cdot 5\text{H}_2\text{O}$  were prepared by dissolving  $\text{Nd}_2\text{O}_3$ ,  $\text{Sm}_2\text{O}_3$ ,  $\text{Gd}_2\text{O}_3$ , or  $\text{Dy}_2\text{O}_3$  in nitric acid in aqueous

\* Corresponding author. Tel./fax: +86 991 8580032.

E-mail address: [jdz@xju.edu.cn](mailto:jdz@xju.edu.cn) (D. Jia).

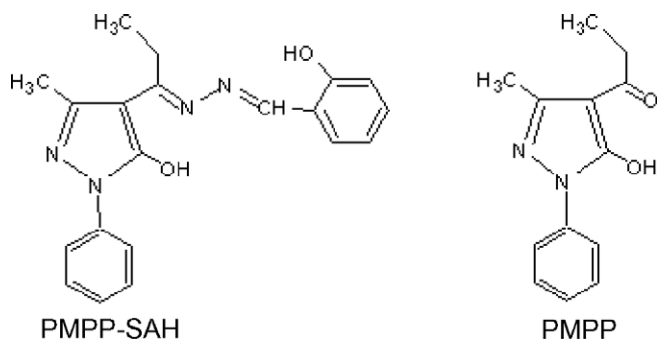


Chart 1.

solutions, then crystallizing the products. 1-Phenyl-3-methyl-4-propionyl-pyrazolone-5 (PMPP) [17] and the salicylic hydrazone (SAH) [18] was synthesized and purified according to the literature method. And the ligand PMPP-SAH was synthesized by refluxing equimolar PMPP and SAH in ethanol for 4 h, adding a few drops of glacial acetic acid as a catalyst. On cooling, the yellow solid obtained was filtered, washed with ethanol, and dried in air. m.p. 178–180 °C. *Anal.* Calc. for  $C_{20}H_{20}N_4O_2$  (Fw: 348.40): C, 68.95; H, 5.79; N, 16.08. Found: C, 69.14; H, 6.14; N, 16.11%. The syntheses of the complexes were performed under hydrothermal condition. A mixture was prepared of  $Ln(NO_3)_3 \cdot xH_2O$  ( $x = 5$ , Ln = Nd, Dy;  $x = 6$ , Ln = Sm, Gd) (0.2 mmol), PMPP-SAH (0.6 mmol), water (10 ml) and EtOH (20 ml), heated in a Teflon-lined stainless steel autoclave for 48 h inside a programmable electric furnace at 130 °C. After cooling the autoclave to room temperature over 48 h, the mixture was filtered off, and then the mixture was allowed to evaporate slowly and reddish brown single crystals suitable for X-ray diffraction were obtained after two weeks. The crystals are stable and no changes were observed after storing under ambient atmosphere. The elemental analyses of the synthesized complexes are summarized in Table 1.

Table 1  
Composition of the products determined by elemental analysis

Complex	%			
	C	H	N	RE
$Nd(C_{13}H_{13}N_2O_3)_3 \cdot 2H_2O \cdot C_2H_5OH$ (1)				
Calc.	53.87	5.40	9.23	15.78
Found	53.44	5.33	9.27	15.35
$Sm(C_{13}H_{13}N_2O_3)_3 \cdot 2H_2O \cdot C_2H_5OH$ (2)				
Calc.	53.51	5.37	9.13	16.34
Found	53.05	5.23	9.49	16.51
$Gd(C_{13}H_{13}N_2O_3)_3 \cdot 2H_2O \cdot C_2H_5OH$ (3)				
Calc.	53.12	5.33	9.06	16.96
Found	53.44	5.33	9.23	17.29
$Dy(C_{13}H_{13}N_2O_3)_3 \cdot 2H_2O \cdot C_2H_5OH$ (4)				
Calc.	52.82	5.30	9.01	17.43
Found	53.07	5.40	9.25	17.08

## 2.2. Instrumentation

The elemental analyses (C, H, N) were determined on a PE-2400 element analyzer. The Re (III) ions were determined by ICP on a Plasma-Spec analyzer. The thermal analyses were carried out on a NETZSCH STA 449C instrument with a heating rate of 20 °C min<sup>-1</sup> in an atmosphere of flowing air. The crystal structures were analyzed using a Bruker Smart 1000 CCD and the SHELXTL 97 crystallographic software package of molecular structure. The fluorescence emission spectra were performed on a HITACHI F-4500 FL Spectrophotometer at room temperature with 380 nm excitation cut-off filter, emission slit at 5 nm and PMT voltage at 400 V. The scan speed was 240 nm/min.

## 2.3. X-ray crystallography

Suitable single crystals of the complexes 1–4 were mounted on a Bruker Smart 1000 CCD diffractometer equipped with graphite monochromated Mo K $\alpha$  ( $\lambda = 0.71073$  Å) radiation. Empirical absorption corrections were applied. The unit cell parameters were determined by least squares refinements of all reflections in all four of the cases. All the structures were solved by direct method and refined by full-matrix least squares on  $F^2$ . All non-hydrogen atoms were refined anisotropically, and hydrogen atoms were located from the difference map, and then added geometrically. All calculations were performed using the SHELXTL97 program package. Crystal data and experimental details for complexes 1–4 are contained in Table 2.

## 3. Results and discussion

We found that the starting ligand PMPP-SAH changed into PMPP in the forming process of complexes 1–4. On the contrary, the PMPP-SAH showed great stability in the presence transition metals and formed polynuclear and supramolecular complexes with special structures in the research by our group. This is probably because the Ln (III) ions induce the activation and cleavage of the carboxamido bond [19]. High coordination numbers of lanthanide elements have advantages in certain organic reactions that can be promoted catalytically in the presence of lanthanide ions. The catalytic roles of lanthanide ions and their complexes in the hydrolytic cleavage of phosphate diesters have been considerably studied. However, so far, the identification of the catalytic mechanism has not been ambiguously rendered [19]. In our work, the ligand PMPP-SAH has been changed into PMPP in the presence of Ln (III) ions.

The four complexes with the general formula Ln (PMPP)<sub>3</sub> · 2H<sub>2</sub>O · C<sub>2</sub>H<sub>5</sub>OH (Ln = Nd (1), Sm (2), Gd (3), Dy (4)) crystallize isostructurally with Tb(PMPP)<sub>3</sub> · 2H<sub>2</sub>O · C<sub>2</sub>H<sub>5</sub>OH reported by Chunhui Huang and coworkers [20]. As shown in Fig. 1, they are built up by the

Table 2  
Crystal data and structure refinement parameters for complexes 1–4

Complexes	1	2	3	4
Empirical formula	C <sub>41</sub> H <sub>49</sub> N <sub>6</sub> O <sub>9</sub> Nd	C <sub>41</sub> H <sub>49</sub> N <sub>6</sub> O <sub>9</sub> Sm	C <sub>41</sub> H <sub>49</sub> N <sub>6</sub> O <sub>9</sub> Gd	C <sub>41</sub> H <sub>49</sub> N <sub>6</sub> O <sub>9</sub> Dy
Formula weight	914.10	920.21	927.11	932.36
Crystal system	monoclinic	monoclinic	monoclinic	monoclinic
<i>T</i> (K)	294(2)	293(2)	293(2)	294(2)
Wavelength (Å)	0.71073	0.71073	0.71073	0.71073
Space group	<i>P</i> 2(1)/ <i>c</i>	<i>P</i> 2(1)/ <i>c</i>	<i>P</i> 2(1)/ <i>c</i>	<i>P</i> 2(1)/ <i>c</i>
<i>a</i> (Å)	17.783(2)	17.7165(11)	17.7165(11)	17.608(4)
<i>b</i> (Å)	12.9749(17)	12.9394(8)	12.9394(8)	12.901(3)
<i>c</i> (Å)	18.438(2)	18.3657(12)	18.3657(12)	18.299(4)
$\alpha$ (°)	90	90	90	90
$\beta$ (°)	102.249(2)	101.874	101.874(10)	101.355(3)
$\gamma$ (°)	90	90	90	90
<i>V</i> (Å <sup>3</sup> )	4157.4(9)	4120.1(5)	4120.1(5)	4075.4(15)
<i>Z</i>	4	4	4	4
Absorption coefficient (mm <sup>-1</sup> )	1.310	1.487	1.671	1.896
Crystal size (mm)	0.22 × 0.18 × 0.12	0.32 × 0.22 × 0.18	0.42 × 0.32 × 0.20	0.26 × 0.24 × 0.20
$\theta$ range for data collection (°)	1.93–26.52	1.94–25.03	1.94–25.03	1.18–26.38
Reflections collected/unique	23 268/8596	21 832/7264	21 789/7260	22 399/8275
Completeness (%)	99.5	99.9	99.9	99.3
Limiting indices	−22 ≤ <i>h</i> ≤ 18, 15 ≤ <i>k</i> ≤ 16, −21 ≤ <i>l</i> ≤ 23	−13 ≤ <i>h</i> ≤ 21, 15 ≤ <i>k</i> ≤ 15, −21 ≤ <i>l</i> ≤ 21	−21 ≤ <i>h</i> ≤ 20, 15 ≤ <i>k</i> ≤ 14, −19 ≤ <i>l</i> ≤ 21	−17 ≤ <i>h</i> ≤ 21, 16 ≤ <i>k</i> ≤ 14, −16 ≤ <i>l</i> ≤ 22
<i>R</i> <sub>int</sub>	0.0248	0.0137	0.0172	0.0345
<i>D</i> <sub>calc</sub> (g cm <sup>-3</sup> )	1.460	1.484	1.495	1.520
Data/restraints/parameters	8596/34/530	7264/36/540	7260/36/540	8275/28/529
<i>F</i> (000)	1876	1884	1892	1900
Goodness-of-fit on <i>I</i>	1.062	1.089	1.035	1.019
Final <i>R</i> indices [ <i>I</i> > 2 $\theta$ ( <i>I</i> )]	<i>R</i> <sub>1</sub> = 0.0282, $\omega R$ <sub>2</sub> = 0.0661	<i>R</i> <sub>1</sub> = 0.0201, $\omega R$ <sub>2</sub> = 0.0556	<i>R</i> <sub>1</sub> = 0.0198, $\omega R$ <sub>2</sub> = 0.0506	<i>R</i> <sub>1</sub> = 0.0303, $\omega R$ <sub>2</sub> = 0.0652
<i>R</i> indices (all data)	<i>R</i> <sub>1</sub> = 0.0456, $\omega R$ <sub>2</sub> = 0.0761	<i>R</i> <sub>1</sub> = 0.0244, $\omega R$ <sub>2</sub> = 0.0584	<i>R</i> <sub>1</sub> = 0.0247, $\omega R$ <sub>2</sub> = 0.0528	<i>R</i> <sub>1</sub> = 0.0511, $\omega R$ <sub>2</sub> = 0.0732
Largest difference in peak and hole (e Å <sup>-3</sup> )	0.859 and −0.503	0.633 and −0.443	0.574 and −0.507	0.791 and −0.625

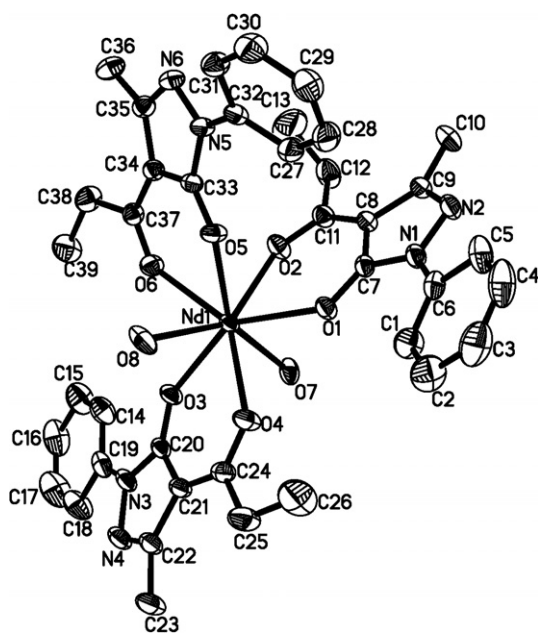


Fig. 1. Crystal structure of a Nd(L)<sub>3</sub> · 2H<sub>2</sub>O · C<sub>2</sub>H<sub>5</sub>OH complex molecule with thermal ellipse at the 30% probability level. The hydrogen atoms and two ethanol molecules being omitted for clarity (Ln = Sm (2), Gd (3) and Dy (4) have the same structure).

mononuclear Ln(PMPP)<sub>3</sub> · 2H<sub>2</sub>O · C<sub>2</sub>H<sub>5</sub>OH compound molecules. The rare earth atoms are coordinated by six oxygen atoms of three bidentate PMPP ligands and the other two oxygen atoms of two coordinated water molecules to complete 8-fold coordinated polyhedron. As far as the average bond lengths between the Ln(III) ion and the pyrazolone oxygen atom, and that between the Ln(III) ion and water oxygen atoms, the former is slightly shorter than the latter, which we can confirm from the data in Table 3. This may be result of the negative charge of the pyrazolone oxygen atom, which could be more strongly coordinated to the Ln(III) ion due to electrostatic effects [20]. Meanwhile, it indicates that the ligand PMPP has better donating properties than the water molecule [21], and the ligand can approach closer to the central ion. The Ln–O bond distances vary over the range 2.372–2.504 Å for compound 1, 2.3493–2.4785 Å for compound 2, 2.3378–2.4491 Å for compound 3 and 2.306–2.432 Å for compound 4 (Table 3). With increasing atomic number of the rare earth atom, the Ln–O bond distances decrease monotonously, which according to excellently with the well-known “lanthanide contraction” [22].

As shown in Fig. 2, the eight oxygen atoms form a square-antiprism coordination polyhedron around the

Table 3  
Selected bond lengths (Å) and angles (°) for complexes 1–4

Complex 1 (Nd)			
Nd(1)–O(1)	2.372(19)	Nd(1)–O(2)	2.440(2)
Nd(1)–O(3)	2.382(19)	Nd(1)–O(6)	2.447(2)
Nd(1)–O(5)	2.410(2)	Nd(1)–O(7)	2.463(2)
Nd(1)–O(4)	2.437(2)	Nd(1)–O(8)	2.504(2)
O(1)–Nd(1)–O(3)	142.46(7)	O(5)–Nd(1)–O(7)	147.05(8)
O(1)–Nd(1)–O(5)	76.63(7)	O(4)–Nd(1)–O(7)	80.74(8)
O(3)–Nd(1)–O(5)	137.97(8)	O(2)–Nd(1)–O(7)	73.27(8)
O(1)–Nd(1)–O(4)	77.23(7)	O(6)–Nd(1)–O(7)	111.35(7)
O(3)–Nd(1)–O(4)	73.04(7)	O(1)–Nd(1)–O(8)	113.64(8)
O(5)–Nd(1)–O(4)	117.29(7)	O(3)–Nd(1)–O(8)	77.88(8)
O(1)–Nd(1)–O(2)	72.62(7)	O(5)–Nd(1)–O(8)	68.95(8)
O(3)–Nd(1)–O(2)	121.36(7)	O(4)–Nd(1)–O(8)	71.48(9)
O(5)–Nd(1)–O(2)	76.81(8)	O(2)–Nd(1)–O(8)	141.83(8)
O(4)–Nd(1)–O(2)	142.48(8)	O(6)–Nd(1)–O(8)	79.64(9)
O(1)–Nd(1)–O(6)	138.98(7)	O(7)–Nd(1)–O(8)	143.53(8)
O(3)–Nd(1)–O(6)	76.71(7)	O(2)–Nd(1)–O(6)	74.40(7)
O(5)–Nd(1)–O(6)	72.64(7)	O(1)–Nd(1)–O(7)	81.53(7)
O(4)–Nd(1)–O(6)	141.65(8)	O(3)–Nd(1)–O(7)	71.61(7)
Complex 2 (Sm)			
Sm(1)–O(6)	2.3493(16)	Sm(1)–O(5)	2.4090(17)
Sm(1)–O(2)	2.3551(16)	Sm(1)–O(3)	2.4248(16)
Sm(1)–O(4)	2.3803(16)	Sm(1)–O(7)	2.4382(18)
Sm(1)–O(1)	2.4079(16)	Sm(1)–O(8)	2.4785(18)
O(6)–Sm(1)–O(2)	142.36(6)	O(5)–Sm(1)–O(7)	73.50(6)
O(6)–Sm(1)–O(4)	76.33(6)	O(3)–Sm(1)–O(7)	111.91(6)
O(2)–Sm(1)–O(4)	138.44(6)	O(6)–Sm(1)–O(8)	114.01(6)
O(6)–Sm(1)–O(1)	76.55(6)	O(2)–Sm(1)–O(8)	77.81(6)
O(2)–Sm(1)–O(1)	73.92(6)	O(4)–Sm(1)–O(8)	69.27(6)
O(4)–Sm(1)–O(1)	116.45(6)	O(1)–Sm(1)–O(8)	71.57(7)
O(6)–Sm(1)–O(5)	73.39(6)	O(5)–Sm(1)–O(8)	141.84(7)
O(2)–Sm(1)–O(5)	120.41(6)	O(3)–Sm(1)–O(8)	79.30(7)
O(4)–Sm(1)–O(5)	77.14(6)	O(7)–Sm(1)–O(8)	143.16(6)
O(1)–Sm(1)–O(5)	142.67(7)	O(5)–Sm(1)–O(3)	74.14(6)
O(6)–Sm(1)–O(3)	139.55(6)	O(6)–Sm(1)–O(7)	80.90(6)
O(2)–Sm(1)–O(3)	76.14(6)	O(2)–Sm(1)–O(7)	71.67(6)
O(4)–Sm(1)–O(3)	73.47(6)	O(4)–Sm(1)–O(7)	146.90(6)
O(1)–Sm(1)–O(3)	141.73(6)	O(1)–Sm(1)–O(7)	80.40(6)
Complex 3 (Gd)			
Gd(1)–O(6)	2.3378(16)	Gd(1)–O(5)	2.3939(17)
Gd(1)–O(2)	2.3485(16)	Gd(1)–O(3)	2.4056(17)
Gd(1)–O(4)	2.3663(16)	Gd(1)–O(7)	2.4113(18)
Gd(1)–O(1)	2.3885(17)	Gd(1)–O(8)	2.4491(19)
O(6)–Gd(1)–O(2)	142.54(6)	O(6)–Gd(1)–O(8)	113.66(6)
O(6)–Gd(1)–O(4)	75.82(6)	O(2)–Gd(1)–O(8)	77.87(6)
O(2)–Gd(1)–O(4)	138.74(6)	O(4)–Gd(1)–O(8)	69.55(6)
O(6)–Gd(1)–O(1)	75.89(6)	O(1)–Gd(1)–O(8)	71.52(7)
O(2)–Gd(1)–O(1)	74.67(6)	O(5)–Gd(1)–O(8)	141.84(7)
O(4)–Gd(1)–O(1)	115.91(6)	O(3)–Gd(1)–O(8)	79.54(7)
O(6)–Gd(1)–O(5)	74.09(6)	O(7)–Gd(1)–O(8)	143.12(6)
O(2)–Gd(1)–O(5)	119.85(6)	O(4)–Gd(1)–O(7)	146.59(6)
O(4)–Gd(1)–O(5)	77.16(6)	O(1)–Gd(1)–O(7)	80.60(6)
O(1)–Gd(1)–O(5)	142.75(6)	O(5)–Gd(1)–O(7)	73.45(6)
O(6)–Gd(1)–O(3)	140.12(6)	O(3)–Gd(1)–O(7)	111.45(6)
O(2)–Gd(1)–O(3)	75.40(6)	O(5)–Gd(1)–O(3)	73.90(6)
O(4)–Gd(1)–O(3)	74.40(6)	O(6)–Gd(1)–O(7)	81.10(6)
O(1)–Gd(1)–O(3)	141.86(6)	O(2)–Gd(1)–O(7)	71.71(6)
Complex 4 (Dy)			
Dy(1)–O(3)	2.306(2)	Dy(1)–O(4)	2.364(2)
Dy(1)–O(1)	2.310(2)	Dy(1)–O(6)	2.380(2)

Table 3 (continued)

Complex 4 (Dy)			
Dy(1)–O(5)	2.332(2)	Dy(1)–O(7)	2.395(2)
Dy(1)–O(2)	2.363(2)	Dy(1)–O(8)	2.432(3)
O(3)–Dy(1)–O(1)	142.29(8)	O(4)–Dy(1)–O(7)	73.44(9)
O(3)–Dy(1)–O(5)	76.00(8)	O(6)–Dy(1)–O(7)	111.68(8)
O(1)–Dy(1)–O(5)	138.78(9)	O(3)–Dy(1)–O(8)	113.80(9)
O(3)–Dy(1)–O(2)	75.04(8)	O(1)–Dy(1)–O(8)	77.96(9)
O(1)–Dy(1)–O(2)	75.49(8)	O(5)–Dy(1)–O(8)	69.33(9)
O(5)–Dy(1)–O(2)	115.04(9)	O(2)–Dy(1)–O(8)	71.66(10)
O(3)–Dy(1)–O(4)	74.86(8)	O(4)–Dy(1)–O(8)	141.79(9)
O(1)–Dy(1)–O(4)	119.06(8)	O(6)–Dy(1)–O(8)	79.22(10)
O(5)–Dy(1)–O(4)	77.79(9)	O(7)–Dy(1)–O(8)	143.06(9)
O(2)–Dy(1)–O(4)	142.81(9)	O(4)–Dy(1)–O(6)	73.77(9)
O(3)–Dy(1)–O(6)	140.80(8)	O(3)–Dy(1)–O(7)	80.70(8)
O(1)–Dy(1)–O(6)	74.94(8)	O(1)–Dy(1)–O(7)	71.71(9)
O(5)–Dy(1)–O(6)	74.90(8)	O(5)–Dy(1)–O(7)	146.78(9)
O(2)–Dy(1)–O(6)	141.97(9)	O(2)–Dy(1)–O(7)	80.60(9)

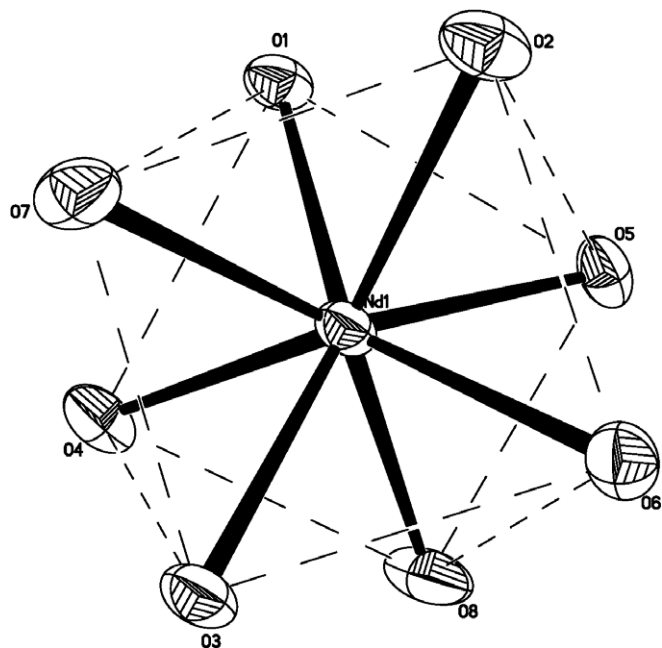


Fig. 2. The coordination polyhedron around the central Neodymium (III) ions (Ln = Sm (2), Gd (3) and Dy (4) have the same structure).

central Nd atom. Four oxygen atoms form the upper plane, and the others form the bottom plane in their coordination polyhedron, respectively. And the dihedral angles

Table 4  
Dihedral angles between the planes

	Complex 1 (Nd)	Complex 2 (Sm)	Complex 3 (Gd)	Complex 4 (Dy)
Plane 1	O2, O3, O6, O7	O1, O8, O6, O4	O1, O8, O6, O4	O1, O7, O6, O4
Plane 2	O1, O8, O5, O4	O7, O2, O3, O5	O2, O7, O5, O3	O2, O8, O5, O3
Dihedral angle	2.4°	2.1°	2.0°	1.9°

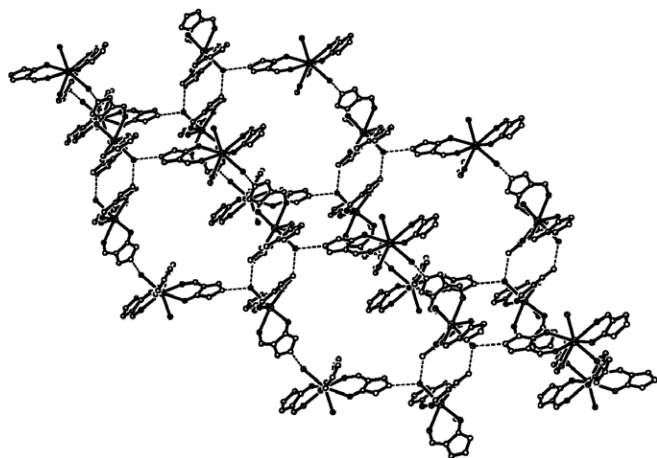


Fig. 3. 3D framework of the  $\text{Nd}(\text{L})_3 \cdot 2\text{H}_2\text{O} \cdot \text{C}_2\text{H}_5\text{OH}$  complexes molecules view along  $b$  axis.

of them are listed in Table 4. These small dihedral angles imply that the two planes are paralleled in each compound.

In the packing arrangement of complex 1, the molecules are stacked into a 3D supramolecular framework through the hydrogen-bonding interactions from the pyrazolone ring and water molecules (Fig. 3). The corresponding data for the H-bonds are listed in Table 5. There are also weak intermolecular interactions in the complexes, which are  $\pi$ – $\pi$  interactions between the pyrazolone ring and benzene ring interiorly. The  $\pi$ – $\pi$  interactions parameters of complexes 1–4 are listed in Table 6.

Table 5  
Some significant interaction parameters and hydrogen bonding parameters for complexes 1–4

D–HA	$d(\text{D–H})$	$d(\text{H} \cdots \text{A})$	$d(\text{D} \cdots \text{A})$	(DHA)
<i>Complex 1</i>				
O7–H7A $\cdots$ N2	0.869	1.974	2.830	168.38
O7–H7B $\cdots$ N6	0.901	1.935	2.824	168.91
O8–H8A $\cdots$ N4	0.883	1.938	2.815	171.61
O8–H8B $\cdots$ O9	0.860	2.075	2.892	158.48
<i>Complex 2</i>				
O7–H7A $\cdots$ N3	0.850	1.988	2.827	168.86
O7–H7B $\cdots$ N5	0.850	1.996	2.834	168.39
O8–H8A $\cdots$ N1	0.850	1.966	2.816	178.72
O8–H8B $\cdots$ O9	0.861	2.175	2.818	131.25
<i>Complex 3</i>				
O7–H7A $\cdots$ N3	0.850	2.004	2.842	168.32
O7–H7B $\cdots$ N5	0.850	2.011	2.849	168.48
O8–H8A $\cdots$ N1	0.850	1.986	2.836	178.27
O8–H8B $\cdots$ O9	0.861	2.181	2.825	131.41
<i>Complex 4</i>				
O7–H7A $\cdots$ N6	0.889	1.964	2.850	174.60
O7–H7B $\cdots$ N4	0.871	1.994	2.857	170.27
O8–H8A $\cdots$ O9	0.919	2.128	2.888	139.38
O8–H8B $\cdots$ N2	0.868	1.971	2.833	171.72

Table 6  
Interactions parameters of complexes 1–4

$\pi$ – $\pi$ Interactions Cg (I)–Res(I)–Cg(J)	Cg–Cg ( $\text{\AA}$ )	$\alpha^\circ$	$\beta^\circ$
<i>Complex 1 (Nd)</i>			
Cg (3) [1] $\rightarrow$ Cg (5)	3.917	14.40	21.00
Cg (3) = N5, N6, C35, C34, C33; Cg (5) = C14, C15, C16, C17, C18, C19			
<i>Complex 2 (Sm)</i>			
Cg (2) [1] $\rightarrow$ Cg (4)	3.9226	15.05	7.77
Cg (2) = N3, N4, C20, C18, C19; Cg (4) = C9, C10, C11, C12, C13, C14			
<i>Complex 3 (Gd)</i>			
Cg (2) [1] $\rightarrow$ Cg (4)	3.9357	15.78	7.87
Cg (2) = N3, N4, C20, C18, C19; Cg (4) = C9, C10, C11, C12, C13, C14			
<i>Complex 4 (Dy)</i>			
Cg (3) [1] $\rightarrow$ Cg (4)	3.932	16.36	7.42
Cg (3) = N5, N6, C35, C34, C33; Cg (4) = C1, C2, C3, C4, C5, C6			

Cg: Centroid,  $\alpha$ : dihedral angle between planes I and J,  $\beta$ : angle Cg (I)  $\rightarrow$  Cg (J) or Cg (I)  $\rightarrow$  Me vector and normal to plane I.

The TG–DTA curves of complexes 1–4 are similar. Some data of thermal analyses are listed in Table 7. The DTA curves of complexes have an endothermic peak around 150 °C and the corresponding TG curves both exhibit a weight loss. This process corresponds to the complexes losing two water molecules and one ethanol molecule. The experimental values are in agreement with the theoretical ones within the experimental error. These results are in accordance with the compositions of the compounds determined by elemental analyses. Meanwhile, they answered for the crystal structure.

The fluorescence spectra of the  $\text{Ln}(\text{PMPP})_3 \cdot 2\text{H}_2\text{O} \cdot \text{C}_2\text{H}_5\text{OH}$  complexes in solid state excited by a 380 nm laser beam are shown in Fig. 4. All complexes exhibit a green emission band peaked at 550 nm which indicates that the fluorescence spectral of complexes is relevant to the structure. However, the spectra of the complexes have a slightly red shift as compared to the ligand, which probably was led by the charge-transfer that was caused by the alternation of the structure of the ligand during the formulation of complex 4 is much stronger than the other complexes in solid state. It probably assigned to the lowest triplet state energy level of ligand and the lowest excited state energy level of  $\text{Dy}^{3+}$  ion is better matched [22].

The emission spectra of the complexes in dimethylformamide (DMF) solution, however, are quite different from those of the powdered samples as shown in Fig. 5. In the same laser beam, the complexes in DMF exhibit a green emission band too, and the fluorescence peaks of all complexes have a blue shift compared with that in solid state. However, the emission peak of complex 3 has a slightly red shift as compared to the other complexes in DMF solution, while this phenomenon had not occurred in solid state. We consider all the difference in emission as the result of the different environment between the two states [24].

Table 7  
Thermal analytical results (TG, DTG, DTA) for the complexes 1–4

Complex	Temperature range (°C)	DTG <sub>max</sub> (°C)	Removed group	Mass loss (%)		Residue (%)		Residue Product
				Found	Calc.	Found	Calc.	
Nd(L) <sub>3</sub> · 2H <sub>2</sub> O · C <sub>2</sub> H <sub>5</sub> OH	104–242	149.9	2H <sub>2</sub> O + C <sub>2</sub> H <sub>5</sub> OH	7.52	9.98	20.00	18.14	Nd <sub>2</sub> O <sub>3</sub>
Sm(L) <sub>3</sub> · 2H <sub>2</sub> O · C <sub>2</sub> H <sub>5</sub> OH	115–226	182.4	2H <sub>2</sub> O + C <sub>2</sub> H <sub>5</sub> OH	8.99	8.92	20.25	19.11	Sm <sub>2</sub> O <sub>3</sub>
Gd(L) <sub>3</sub> · 2H <sub>2</sub> O · C <sub>2</sub> H <sub>5</sub> OH	89–208	124.4	2H <sub>2</sub> O + C <sub>2</sub> H <sub>5</sub> OH	8.20	8.85	16.38	19.62	Gd <sub>2</sub> O <sub>3</sub>
Dy(L) <sub>3</sub> · 2H <sub>2</sub> O · C <sub>2</sub> H <sub>5</sub> OH	96–206	138.7	2H <sub>2</sub> O + C <sub>2</sub> H <sub>5</sub> OH	8.28	8.80	17.81	20.15	Dy <sub>2</sub> O <sub>3</sub>

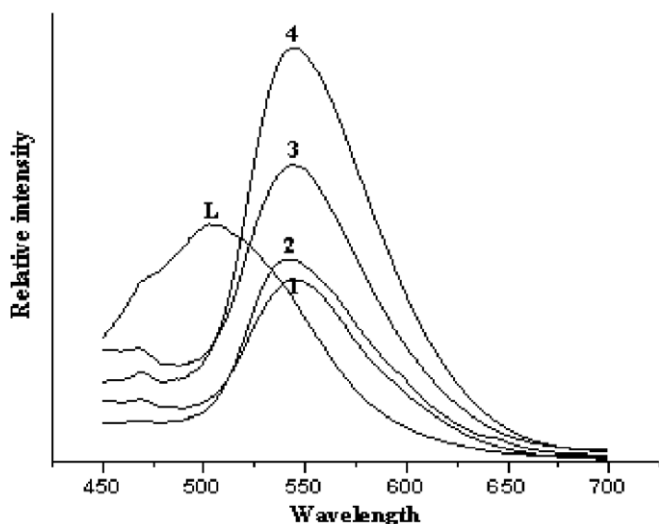


Fig. 4. Room temperature fluorescence spectra of Ln(PMPP)<sub>3</sub> · 2H<sub>2</sub>O · C<sub>2</sub>H<sub>5</sub>OH in solid state excited by a 380 nm laser beam.

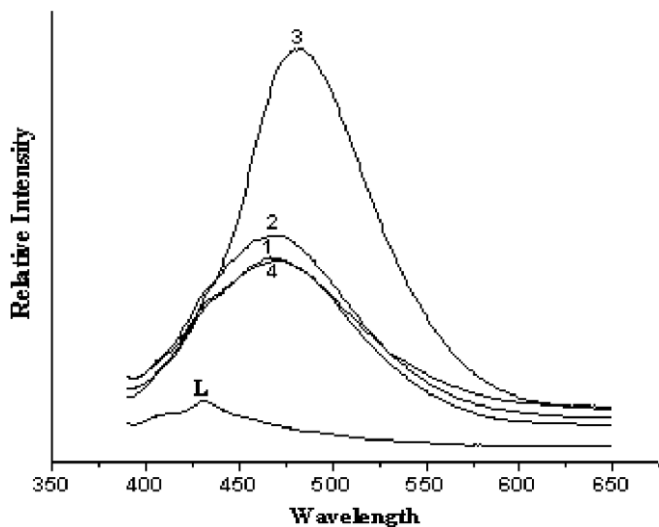


Fig. 5. The fluorescence emission spectra of Ln(PMPP)<sub>3</sub> · 2H<sub>2</sub>O · C<sub>2</sub>H<sub>5</sub>OH in DMF solution excited by a 380 nm laser beam.

## Acknowledgments

This work was supported by the National Natural Science Foundation of China (Nos. 20366005 and 20462007), the Scientific Research Foundation in Xinjiang

Educational Institutions (XJEDU2005S01) and the Young Scholar Science Foundation of Xinjiang University (QN040107).

## Appendix A. Supplementary material

CCDC 613546, 613547, 613548 and 613549 contain the supplementary crystallographic data for this paper. These data can be obtained free of charge via <http://www.ccdc.cam.ac.uk/conts/retrieving.html>, or from the Cambridge Crystallographic Data Centre, 12 Union Road, Cambridge CB2 1EZ, UK; fax: (+44) 1223-336-033; or e-mail: deposit@ccdc.cam.ac.uk. TG–DTA plots for 1–4 are available from the authors on request. Supplementary data associated with this article can be found, in the online version, at doi:10.1016/j.ica.2006.10.010.

## References

- [1] R.B. Martin, F.S. Richardson, *Q. Rev. Biophys.* 12 (1979) 181.
- [2] R.B. Laufer, *Chem. Rev.* 87 (1987) 901.
- [3] C. Piguet, G. Hopfgartner, A.F. Williams, J.-C.G. Bünzli, *J. Chem. Soc., Chem. Commun.* (1995) 491.
- [4] M. Shibusaki, H. Sasai, T. Arai, *Angew. Chem., Int. Ed. Engl.* 36 (1997) 1236.
- [5] C.A. Parker, *Photoluminescence of Solutions*, Elsevier, Amsterdam, 1968, pp. 470.
- [6] S. Umetani, H. Freiser, *Inorg. Chem.* 26 (1987) 3179.
- [7] F.S. Richardson, *Chem. Rev.* 82 (1982) 541.
- [8] M.F. Iskander, L. Sayed, A.F.M. Hefny, S.E. Zayan, *J. Inorg. Nucl. Chem.* 38 (1976) 2209.
- [9] H. Adams, D.E. Fenton, G. Minardi, E. Mura, M. Angelo, *Inorg. Chem. Commun.* 3 (2000) 24.
- [10] Z.Y. Yang, R.D. Yang, F.S. Li, K.B. Yu, *Polyhedron* 19 (2000) 2599.
- [11] B.A. Uzoukwu, P.U. Adiukwu, S.S. Al-Juaid, P.B. Hitchcock, J.D. Smith, *Inorg. Chim. Acta* 250 (1996) 173.
- [12] N. Adhikari, S. Chaudhuri, R.J. Butcher, N. Saha, *Polyhedron* 18 (1999) 1323.
- [13] N. Raman, A. Kulandaisamy, A. Shunmugasundaram, K. Jayasubramanian, *Transition Met. Chem.* 26 (2001) 131.
- [14] L. Zhang, L. Liu, D.Z. Jia, G.C. Xu, K.B. Yu, *Inorg. Chem. Commu.* 7 (2004) 1306.
- [15] L. Zhang, L. Liu, D.Z. Jia, K.B. Yu, *Struct. Chem.* 15 (2004) 327.
- [16] G.C. Xu, L. Zhang, L. Liu, G.F. Liu, D.Z. Jia, *Thermochim. Acta* 429 (2005) 31.
- [17] B.S. Jensen, *Acta Chem. Scand.* 13 (1959) 1668.
- [18] R.Q. Huang, H.L. Wang, J. Zhou, *Preparation of Organic Intermediates*, Chemistry Industrial Press, China, 1997, p. 109.
- [19] H.W. Hou, Y.L. Wei, Y.L. Song, Y.T. Fan, Y. Zhu, *Inorg. Chem.* 43 (2004) 1323.

- [20] D.J. Zhou, Q. Li, C.H. Huang, G.Q. Yao, et al., *Polyhedron* 16 (1996) 1381.
- [21] (a) R. Reisfeld, C.K. Jorgensen, *Lasers and Excited States of Rare Earths*, Springer, Berlin, 1977;  
(b) S. Amine, M. Botta, M. Fasano, E. Terreno, *Chem. Soc. Rev.* 27 (1998) 19.
- [22] C.H. Huang, *Rare Earth Coordination Chemistry*, Science Press, Moscow, 1997, p. 363.
- [23] B.A. Uzoukwu, *Spectrochim. Acta A* 51 (1995) 1081.
- [24] H.Y. Chao, L.Y. Wang, X.Y. Wang, J.R. Li, D.B. Nie, W.F. Fu, S. Gao, *J. Solid State Chem.* 177 (2004) 3735.